Available online at www.sciencedirect.com
ScienceDirect
Geochimica et Cosmochimica Acta 75 (2011) 887–904
Geochimica et Cosmochimica Acta
www.elsevier.com/locate/gca

Experimentally determined biomediated Sr partition coefficient for dolomite: Significance and implication for natural dolomite

Mónica Sánchez-Román [a,b,c,*], Judith A. McKenzie [a], Angela de Luca Rebello Wagener [d], Christopher S. Romanek [b,e], Antonio Sánchez-Navas [f], Crisógono Vasconcelos [a]

[a] ETH-Zürich, Geological Institute, 8092 Zürich, Switzerland
[b] NASA Astrobiology Institute and Department of Geology, University of Georgia, Drawer E, Aiken, SC 29808, USA
[c] Centro de Astrobiología, INTA-CSIC, Ctra Ajalvir Km 4, Torrejón de Ardoz, 28850 Madrid, Spain
[d] Department of Chemistry, PUC, 22453-900 Rio de Janeiro, Brazil
[e] Department of Earth and Environmental Sciences, University of Kentucky, Lexington, KY 40506, USA
[f] Departamento de Mineralogía y Petrología, Facultad de Ciencias, Universidad de Granada, 18071 Granada, Spain

Received 18 February 2010; accepted in revised form 11 November 2010; available online 18 November 2010

Abstract

Two strains of moderately halophilic bacteria were grown in aerobic culture experiments containing gel medium to determine the Sr partition coefficient between dolomite and the medium from which it precipitates at 15 to 45 °C. The results demonstrate that Sr incorporation in dolomite does occur not by the substitution of Ca, but rather by Mg. They also suggest that Sr partitioning between the culture medium and the minerals is better described by the Nernst equation ($D_{Sr}^{dol} = Sr_{dol}/Sr_{bmi}$), instead of the Henderson and Kracek equation ($D_{Sr}^{dol} = (Sr/Ca)_{dol}/(Sr/Ca)_{solution}$. The maximum value for D_{Sr}^{dol} occurs at 15 °C in cultures with and without sulfate, while the minimum values occur at 35 °C, where the bacteria exhibit optimal growth. For experiments at 25, 35 and 45 °C, we observed that D_{Sr}^{dol} values are greater in cultures with sulfate than in cultures without sulfate, whereas D_{Sr}^{dol} values are smaller in cultures with sulfate than in cultures without sulfate at 15 °C.

Together, our observations suggest that D_{Sr}^{dol} is apparently related to microbial activity, temperature and sulfate concentration, regardless of the convention used to assess the D_{Sr}^{dol}. These results have implications for the interpretation of depositional environments of ancient dolomite. The results of our culture experiments show that higher Sr concentrations in ancient dolomite could reflect microbial mediated primary precipitation. In contrast, previous interpretations concluded that high Sr concentrations in ancient dolomites are an indication of secondary replacement of aragonite, which incorporates high Sr concentrations in its crystal lattice, reflecting a diagenetic process.

1. INTRODUCTION

In 1962, Ingerson asserted that the "problem of the origin of dolomite is one of the most fascinating, as well as one the most important in all of geochemistry or in sedimentary petrology". Dolomite is a common sedimentary rock, being ever-present in the geologic record from the Precambrian to the Pleistocene (Weber, 1964). Despite the fact that present oceans are supersaturated with respect to dolomite; it does not commonly form in modern sedimentary environments, and it has been nearly impossible to precipitate dolomite in the laboratory at Earth's surface temperatures and pressure (Land, 1998). Adding to the problem is the fact that dolomite is a stable carbonate phase at Earth surface temperatures and pressures (Zen, 1960). In the last decade, a

* Corresponding author. Present address: Centro de Astrobiología, INTA-CSIC, Ctra Ajalvir Km 4, Torrejón de Ardoz, 28850 Madrid, Spain. Tel.: + 34 91 5206429; fax: +34 91 5201074.
E-mail address: msanz78@gmail.com (M. Sánchez-Román).

0016-7037/$ - see front matter © 2010 Elsevier Ltd. All rights reserved.
doi:10.1016/j.gca.2010.11.015

microbial origin has been added to the list of formation mechanisms for dolomite (Vasconcelos and McKenzie, 1997). There is a strong tendency to reduce the problem by defining the particular solution that will overcome the well-known reluctance of dolomite to nucleate and grow at 25 °C or thereabout. Although the oxygen-isotope fractionation factor for dolomite at low temperatures has been calculated (Vasconcelos et al., 2005), as well as the recognition of distinctive carbon isotopes values (Kelts and McKenzie, 1982; Vasconcelos and McKenzie, 1997), these indicators only imply temperature of precipitation or the active microbial processes producing bicarbonate ions, respectively, but they do not unambiguously identify the parent-water composition or its source.

There is a fairly extensive literature dealing with the abundance of trace elements in carbonate minerals, sediments, and rocks, but experimental data on the incorporation of trace elements in dolomite are relatively rare. Numerous authors have studied the concentration of Sr in dolomite (Weber, 1964; Behrens and Land, 1972; Land et al., 1975; Katz and Mathews, 1977; Land, 1980, 1985; Baker and Burns, 1985; Vahrenkamp and Swart, 1990; amongst others). The primary objective of such research has been to use the Sr content to constrain the environment of dolomite formation. However, ambiguity in interpreting trace element values in dolomites revolves around a number of factors, the most important of which are: (1) our inability to synthesize dolomite in the laboratory and, thus, measure partition coefficients under controlled conditions at low temperatures (e.g., 25 °C), composition and (2) difficulties in quantifying the volumes of various diagenetic fluids and their chemical overprints, which alter crystal chemistry of natural dolomite over time (Vahrenkamp and Swart, 1990). For these reasons, the partition coefficient for the incorporation of Sr into dolomite (D_{Sr}^{dol}) is not well constrained. The range of D_{Sr}^{dol} proposed in the literature (Behrens and Land, 1972; Katz and Mathews, 1977; Baker and Burns, 1985; Vahrenkamp and Swart, 1990) yield uncertainties in the predicted relationship between the Sr contents of fluids and dolomites. Hence, because it is not known what the typical Sr content of a dolomite from a given environment should be, the use of this trace element has been limited in geochemical studies (Land, 1980). Despite this problem, the Sr content of dolomite has been used as a proxy to define diagenetic environments.

Recently, Sánchez-Román et al. (2008, 2009a,b) have shown that moderately halophilic aerobic bacteria (MHAB) mediate the precipitation of dolomite at room temperature. Further, they have demonstrated that sulfate ions do not hinder the formation of dolomite (Sánchez-Román et al., 2009b). They proposed that degradation of organic matter by MHAB simultaneously increases the carbonate alkalinity to produce local supersaturation in the micro-environment around bacterial surfaces capable of overcoming the low-temperature kinetic barriers to precipitate dolomite. Unfortunately this mechanism fails to explain why inorganic dolomite cannot be synthesized in the laboratory at room temperature. The goal of this study is to define, using MHAB cultures experiments, the Sr partition coefficient for microbial dolomite precipitated under controlled laboratory conditions and compare the results with the available published data. The aim of this work is to better understand the microbial and geochemical signals recorded in Recent and ancient dolomite, precipitated under oxic conditions, and evaluate if these signals can be traced throughout the geological record. Certainly, the incorporation of a biological factor into the geochemical equation will add a unique understanding of the metal incorporation processes during biomineralization. A better understanding of these parameters will help to reconstruct fossil and modern environments of dolomite formation providing bio-geochemical information at the interface between biology and geology.

In the present study, we report for the first time the results of a series of *Bacillus* and *Halomonas* culture experiments on the co-precipitation of Sr with dolomite over the temperature range from 15 to 45 °C, and two sulfate concentrations (0 and 58 mM). We propose partition coefficients for Sr in dolomite as a function of temperature, microbial activity and sulfate concentration. That permits the microbial origin for dolomite to be evaluated in modern and ancient environments. These data provide an alternative explanation for the long-standing Dolomite Problem and dolomitization processes.

2. MATERIALS AND METHODS

2.1. Microorganisms

Two species of halophilic bacterium were used in this study:

(1) *Virgibacillus marismortui* AJ009793: a gram positive rod, height = 2–4 μm and width = 0.8–1.2 μm, endospore-forming, chemoorganotrophic and strictly aerobic bacterium. Growth occurs in solutions of 5–25% (w/v) total salts and at temperatures between 15 and 50 °C, with optimal growth at 10% (w/v) and 37 °C (Arahal et al., 1999).
(2) *Halomonas meridiana* ACAM 246 (= UQM 3352): a gram-negative rod, height = 0–3.6 μm and width = 0.5-0.7 0.5–0.7 μm, non-spore-forming, chemoorganotrophic and strictly aerobic bacterium. It optimally grows in solutions of 1–3% NaCl and temperatures between 28 and 40 °C. The maximum salt tolerance is 20–25% NaCl and the maximum growth temperature is 45 °C (James et al., 1990).

Both species are moderately halophilic bacteria. Because they grow under widely changing saline concentrations, these microorganisms are highly useful to determine how the ionic composition of the environment affects the bacterial precipitation of minerals.

2.2. Culture media

D-1 medium was used in the culture experiments; it has the following composition, (%, w/v): 1% yeast extract; 0.5% proteose peptone; 0.1% glucose; 3.5% NaCl; 84 mM Mg; 11 mM Ca and 0.23 mM Sr to get a final concentration of

20 ppm Sr. The medium was modified by adding 58 mM SO_4 in some experiments. To obtain a solid medium, 20 g/l of Bacto-Agar was added. The pH was adjusted to ~7.2 (see Table 1) with 0.1 M KOH and the solution was sterilized at 121 °C for 20 min.

Our culture experiments were designed to simulate the specific Earth's surface conditions (like shallow marine/lacustrine sediments rich in organic matter, biofilms and/or mats, pore-space) where precipitation of dolomite occurs.

2.3. Crystal formation and mineralogy

Virgibacillus marismortui and *H. meridiana* were surface-inoculated onto solid media having two sulfate concentrations (0 and 58 mM). All the cultures were incubated aerobically at 15, 25, 35 and 45 °C. The cultures were periodically examined for the presence of precipitates using an optical microscope. Each experiment was carried out in triplicate. Control experiments, consisting of uninoculated cultures and cultures inoculated with dead bacterial cells, were included for all experimental conditions.

The crystals formed in the bacterial cultures were isolated, purified and identified. Struvite crystals were extracted from media using a small spatula; they were washed with distilled water and then dried at 37 °C. Carbonate crystals were removed by cutting out pieces of media, which were placed in boiling water to dissolve the agar. The resulting suspension was resuspended and washed in distilled water to free crystals of impurities. This treatment did not alter the morphology of crystals, as observed by comparison with precipitates embedded in media. The carbonate crystals were then dried at 37 °C.

Crystals were examined by X-ray diffraction analysis (Scintag). From the d_{104} peak of the diffraction spectrum, the Mg:Ca ratio of dolomite was calculated (after Lumsden, 1979). Dolomite peaks and superstructure reflections were identified and labelled by *hkl* indices. Superstructure reflections are indicated by odd-numbers. See Appendix Fig. 1. The peak broadening measure for 104 reflection in the carbonate precipitates was performed using full width at half maximum (FWHM) as a measure of pure diffraction broadening after instrumental factors correction and $K\alpha_2$ stripping (Klug and Alexander, 1973; Martín, 2004). A LEO 1530 scanning electron microscope (SEM), equipped with an electron dispersive detector (EDS), was used for imaging and elemental analysis of single crystals.

2.4. Sample preparation for elemental analysis

Mineral separates were prepared from the solid retrieved from each experiment. Crystals of struvite were collected using binocular microscope and a brush to separate them from carbonate minerals, as they are well distinguishable by shape, color and size. The remaining solid (mainly hydromagnesite and dolomite) was sonicated for one day. As hydromagnesite crystals were 50–200 μm in diameter and dolomite crystals were 5–30 μm in diameter, these two minerals were separated in the following way: the samples were washed over a 200 μm sieve to retrieve the largest hydromagnesite crystals. The residue was sequentially washed over 100, 60, 40, 20 and 10 μm sieves until single crystals of dolomite remained. Individual dolomite crystals (diameter: 5–30 μm) were collected with a brush using a binocular microscope and they were mounted on a quartz-slide and fixed with a clean impurity free nail lacquer.

The gel medium (agar), below the bacterial mass (bacteria-medium interface, "bmi', site for mineral precipitation), was cut into 10 × 7 mm pieces. The pieces of agar were dried at room temperature for two weeks, and then mounted on quartz-slides and fixed with a clean impurity free nail lacquer.

Table 1
Times required for microbial growth and biomineral precipitation.

Bacterial strain	T (°C)	SO_4^{2-} (mM)	pH[a]	pH[b]	Time (days)		
					Growth	Starting precipitation	Widespread precipitation
V. marismortui	15	0	7.2	8.5		6	13
V. marismortui	15	0	7.2	8.5		6	13
V. marismortui	25	0	7.2	8.5	2	4	12
V. marismortui	35	0	7.0	8.5	1	3	8
V. marismortui	45	0	7.3	9	1	3	7
V. marismortui	15	56	7.2	8.5	3	7	13
V. marismortui	25	56	7.0	8.5	2	4	12
V. marismortui	35	56	7.2	9.5	1	3	9
V. marismortui	45	56	7.1	9.5	1	3	8
H. meridiana	15	0	7.4	8.5	3	10	14
H. meridiana	25	0	7.0	8.5	2	5	12
H. meridiana	35	0	7.3	8.5	1	3	9
H. meridiana	45	0	7.2	8.5	1	2	6
H. meridiana	15	56	7.4	8.5	3	4	14
H. meridiana	25	56	7.0	8.5	1	4	12
H. meridiana	35	56	7.2	9	2	3	8
H. meridiana	45	56	7.2	9	1	2	6

[a] Starting pH in the medium.
[b] Final pH in cultures with living bacteria.

2.5. Laser-ablation inductively-coupled mass-spectrometry analysis

Laser ablation-inductively coupled plasma mass spectrometry (LA-ICP-MS) analyses were performed at the Institute for Isotope Geochemistry and Mineral Resources, ETH–Zürich, using an ELAN 6000 quadruple ICP-MS mass spectrometer equipped with an Excimer 193 nm ArF laser, as described in Guenther et al. (1997). For the measurement of dolomite crystals and dry media, the 193 nm laser was calibrated using a NIST 610 certified glass standard reference material. Up to 10 samples were loaded with the standard and put on the stage of a modified petrographic microscope. Pulse energy (70–80 mJ) was adjusted according to sampling resolutions, usually 40 μm spot diameter for media and 10–14 μm spot diameter for dolomite crystals. Uniform transport efficiency from the ablation cell to the ICP-MS was ensured by using a low internal volume ablation cell and a minimum length for the tubing. The aerosol produced by ablation was transferred to the ICP-MS, using a mixed He–Ar carrier gas (Guenther and Heinrich, 1999), which enables simultaneous determination of elements in a matrix (±100 wt%) to a few parts per billions (ppb) in a single analysis. The ICP-MS operating conditions were optimized using continuous ablations of NIST glass, providing maximum sensitivity. Transient signals of seven isotopes were measured with one point peak and 10 ms dwell time per peak (see Appendix Table 1). Other parameters used for the experiment are shown in the Appendix Table 1. LA-ICP-MS provides element intensity measurements, which were converted to concentrations by dividing the intensity of a particular analyte (e.g., Sr) to concentration for comparison to the reference material (NIST SRM 610) and developing calibration curves. Limits of detection was estimated for each element, using three times the standard deviation of the background measurement (Longerich et al., 1996).

3. RESULTS

3.1. Culture experiments

In all culture experiments, *V. marismortui* and *H. meridiana* precipitated carbonate and phosphate minerals. Table 1 shows the times required for *V. marismortui* and *H. merididana* to grow, for the start of precipitation and for the production of widespread precipitation; the original pH in the media and the final pH in the cultures with living bacteria. In all of the culture experiments, the time required for the initiation and widespread precipitation decreased with increasing temperature. A significant rise in pH occurred in the culture media with living bacteria, from an original pH of ~7.2 up to ~9.5. No precipitation of minerals was observed and no changes in pH (pH ~7) were detected in the control experiments.

Dolomite [$CaMg(CO_3)_2$], hydromagnesite [$Mg_5(CO_3)_4(OH)\cdot 4H_2O$] and struvite [$NH_4Mg(PO_4)\cdot 6H_2O$)] co-precipitated in all culture experiments. The amount of crystals precipitated was higher in experiments conducted at 35–45 °C than at 15–25 °C. The amount of hydromagnesite and struvite was minor compared to the amount of dolomite. Struvite crystals formed mainly at the edge of the individual bacterial masses. In general, carbonates (dolomite and hydromagnesite) began to precipitate at the edge of the bacterial mass forming a ring, which grew wider with incubation time.

Table 2 shows the composition of the dolomite precipitated in the various experiments, as determined by X-ray diffraction analysis. The dolomite is calcium-rich (Ca-dolomite) and ordered, being nearly stoichiometric in the experiments with *V. marismortui* conducted at 35 and 45 °C (see Table 2 and Appendix Fig. 1). The presence of superstructure reflections indicates that these biomediated precipitates are composed of ordered dolomite (Appendix Fig. 1). Note that in some of the X-ray patterns, the superstructure reflections are weak indicating minor

Table 2
XRD data and composition of dolomite from culture experiments.

Culture	T (°C)	SO_4^{2-} (mM)	d_{104} (Å)	Formula[a] for dolomite	FWHM (°2θ)[b]
V. marismortui	15	0	2.916	$Ca_{0.60}Mg_{0.40}(CO_3)$	0.94
V. marismortui	25	0	2.902	$Ca_{0.55}Mg_{0.45}(CO_3)$	1.12
V. marismortui	35	0	2.893	$Ca_{0.53}Mg_{0.47}(CO_3)$	1.10
V. marismortui	45	0	2.891	$Ca_{0.52}Mg_{0.48}(CO_3)$	1.08
V. marismortui	15	56	2.910	$Ca_{0.58}Mg_{0.42}(CO_3)$	1.01
V. marismortui	25	56	2.902	$Ca_{0.55}Mg_{0.45}(CO_3)$	0.95
V. marismortui	35	56	2.904	$Ca_{0.56}Mg_{0.44}(CO_3)$	0.98
V. marismortui	45	56	2.894	$Ca_{0.53}Mg_{0.47}(CO_3)$	1.10
H. meridiana	15	0	2.907	$Ca_{0.58}Mg_{0.42}(CO_3)$	1.00
H. meridiana	25	0	2.910	$Ca_{0.58}Mg_{0.42}(CO_3)$	0.97
H. meridiana	35	0	2.909	$Ca_{0.58}Mg_{0.42}(CO_3)$	0.92
H. meridiana	45	0	2.905	$Ca_{0.57}Mg_{0.43}(CO_3)$	1.03
H. meridiana	15	56	2.945	$Ca_{0.60}Mg_{0.40}(CO_3)$	0.83
H. meridiana	25	56	2.912	$Ca_{0.59}Mg_{0.41}(CO_3)$	0.90
H. meridiana	35	56	2.901	$Ca_{0.55}Mg_{0.45}(CO_3)$	0.93
H. meridiana	45	56	2.902	$Ca_{0.55}Mg_{0.45}(CO_3)$	1.13

[a] The formulas were obtained from d_{104} peak of the diffraction spectra, according to Lumsden (1979).
[b] The FWHM (full width at half maximum) values are around 1° (2θ) in all the studied samples and in some cases broad peaks show shoulders which indicate that there is some compositional heterogeneity resulting from the existence of intergrowths or zoned crystals composed of diverse double (Ca, Mg) carbonate phases as Ca-dolomite, protodolomite and/or dolomite (see notes in the Appendix).

ordering (dolomite precipitated in cultures at 15 °C), whereas in some others are stronger indicating cation ordering (dolomite precipitated in cultures at 25, 35 and 45 °C).

No differences in morphology or crystal shape were observed with respect to bacterium species, temperature or sulphate concentration. In all culture experiments dolomite was produced with spheroidal and dumbbell morphology, up to 20–30 μm in diameter (Fig. 1).

Medium (bacteria-medium interface, "bmi", site of dolomite precipitation) and single crystals of dolomite were analysed by LA-ICP-MS to determine the elemental composition of Ca, Mg and Sr. The results for dolomite crystals from *V. marismortui* and *H. meridiana* experiments are reported in the Appendix (Tables 2 and 3, respectively), and the results for *V. marismortui* and *H. meridiana* bacteria-medium interface ("bmi") are reported in the Appendix (Tables 4 and 5, respectively).

3.2. Elemental analysis of Ca, Mg and Sr

The elemental data for the dolomite and the bacteria-medium interface ("bmi", site of dolomite precipitation)

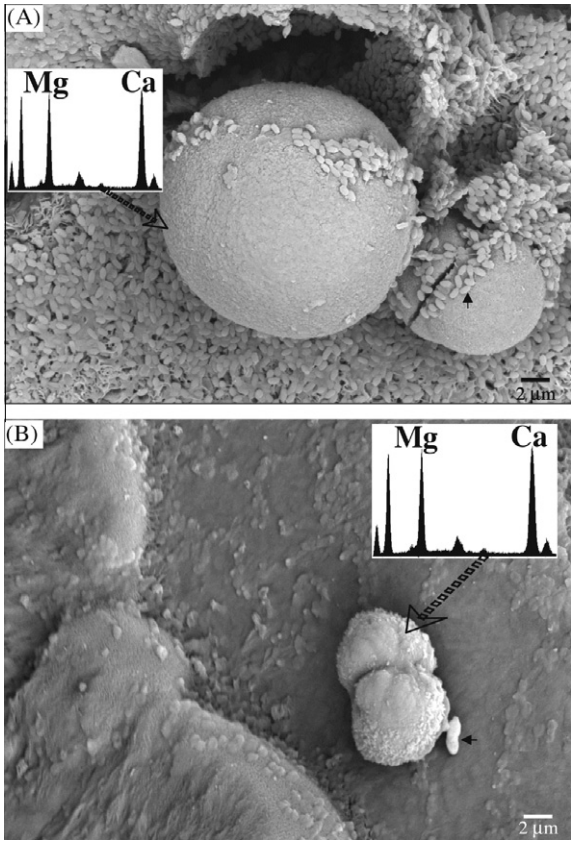

Fig. 1. SEM photomicrographs showing the morphology of biogenic dolomite precipitated in culture experiments. (A) Spherulites of dolomite formed in *H. merididana* cultures without sulfate at 25 °C. Bacteria are closely related to dolomite (arrow). Microphotograph taken from Sánchez-Román et al. (2008). (B) Dolomite dumbbell covered with fine layer of microcrystals formed in *V. marismortui* culture with sulfate at 35 °C. A rod shape bacterium (arrow) is closely related to the dolomite dumbbell that precipitated in this culture. Microphotograph taken from Sánchez-Román et al. (2009b). EDS spectra indicate mineralogy of the dolomite samples.

Table 3
Average Sr concentration and Mg/Ca, Sr/Ca and (Mg + Sr)/Ca molar ratios for "bmi"(bacterium medium interface) in *V. marismortui* and *H. meridiana* cultures without and with sulfate.

T (°C)	"bmi" in *V. marismortui* cultures								"bmi" in *H. meridiana* cultures							
	Without sulfate				With sulfate				Without sulfate				With sulfate			
	Sr (ppm)	Mg/Ca	Sr/Ca	(Mg + Sr)/Ca	Sr(ppm)	Mg/Ca	Sr/Ca	(Mg + Sr)/Ca	Sr(ppm)	Mg/Ca	Sr/Ca	(Mg + Sr)/Ca	Sr (ppm)	Mg/Ca	Sr/Ca	(Mg + Sr)/Ca
15	86 ± 0.07	1.88 ± 0.54	0.044 ± 0.44	1.93 ± 0.53	145 ± 0.20	1.74 ± 0.33	0.036 ± 0.33	1.77 ± 0.33	74 ± 0.07	1.60 ± 0.06	0.036 ± 0.07	1.70 ± 0.09	123 ± 0.04	1.58 ± 0.19	0.038 ± 0.14	1.62 ± 0.19
25	160 ± 0.10	1.40 ± 0.34	0.046 ± 0.21	1.45 ± 0.34	207 ± 0.03	1.48 ± 0.11	0.045 ± 0.15	2.53 ± 0.11	85 ± 0.17	2.80 ± 0.19	0.045 ± 0.05	2.85 ± 0.33	165 ± 0.09	2.69 ± 0.04	0.045 ± 0.02	2.73 ± 0.03
35	156 ± 0.23	2.65 ± 0.29	0.051 ± 0.29	2.70 ± 0.29	250 ± 0.09	2.91 ± 0.23	0.054 ± 0.21	2.97 ± 0.23	162 ± 0.28	3.13 ± 0.23	0.048 ± 0.12	3.18 ± 0.42	252 ± 0.04	2.94 ± 0.04	0.055 ± 0.06	3.00 ± 0.04
45	171 ± 0.03	2.38 ± 0.13	0.051 ± 0.19	2.43 ± 0.13	245 ± 0.04	2.50 ± 0.15	0.054 ± 0.05	2.55 ± 0.15	127 ± 0.16	2.54 ± 0.33	0.051 ± 0.07	2.59 ± 0.45	211 ± 0.08	2.18 ± 0.17	0.053 ± 0.12	2.23 ± 0.17

Note: $n = 3$, average values calculated from Tables 4 and 5 in the Appendix.

Table 4
Average Sr concentration and Mg/Ca, Sr/Ca and (Mg + Sr/Ca) molar ratios for "bmi" (bacterium medium interface) of both *V. marismortui* and *H. meridiana* cultures without and with sulfate.

T (°C)	"bmi" in cultures without sulfate				"bmi" in cultures with sulfate			
	Sr (ppm)	Mg/Ca	Sr/Ca	(Mg + Sr)/Ca	Sr (ppm)	Mg/Ca	Sr/Ca	(Mg + Sr)/Ca
15	80 ± 0.1	1.74 ± 0.11	0.040 ± 0.14	1.82 ± 0.08	134 ± 0.11	1.66 ± 0.06	0.037 ± 0.03	1.69 ± 0.06
25	123 ± 0.43	2.10 ± 0.47	0.045 ± 0.01	2.15 ± 0.46	186 ± 0.15	2.58 ± 0.41	0.045 ± 0	2.63 ± 0.05
35	159 ± 0.02	2.89 ± 0.11	0.049 ± 0.04	2.94 ± 0.11	251 ± 0.05	2.93 ± 0.007	0.054 ± 0.01	2.98 ± 0.007
45	149 ± 0.20	2.46 ± 0.04	0.051 ± 0	2.51 ± 0.04	228 ± 0.10	2.34 ± 0.09	0.054 ± 0.01	2.39 ± 0.09

Note: $n = 2$, average values calculated from Table 3.

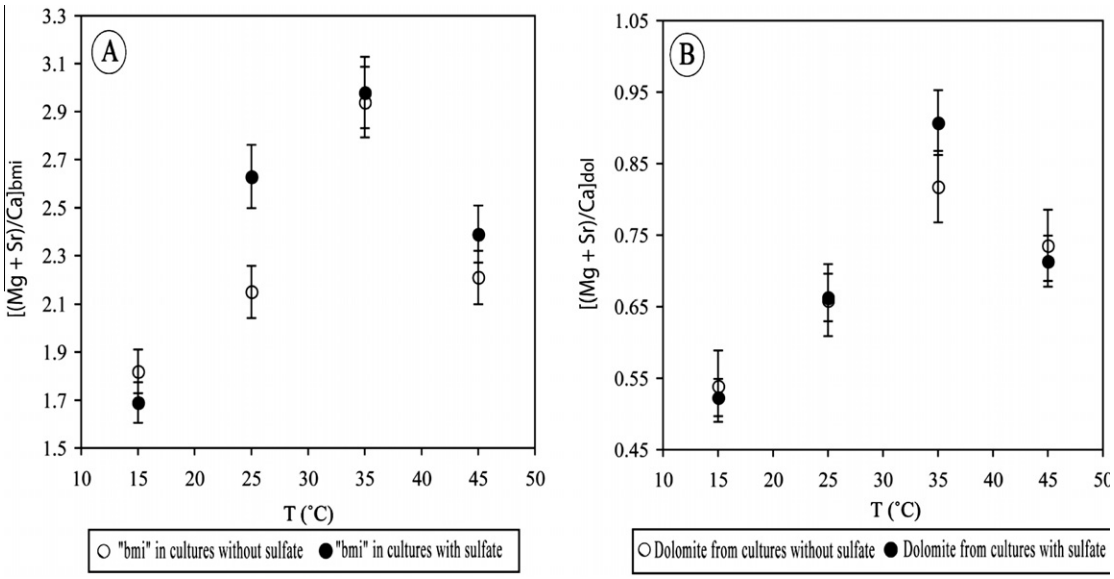

Fig. 2. (A) Average values for (Mg + Sr)/Ca molar ratios in the bacteria-medium interface ('bmi', site of mineral precipitation) from culture experiments with and without sulfate. (B) Average values for (Mg + Sr)/Ca molar ratios in dolomite precipitates from culture experiments with and without sulfate.

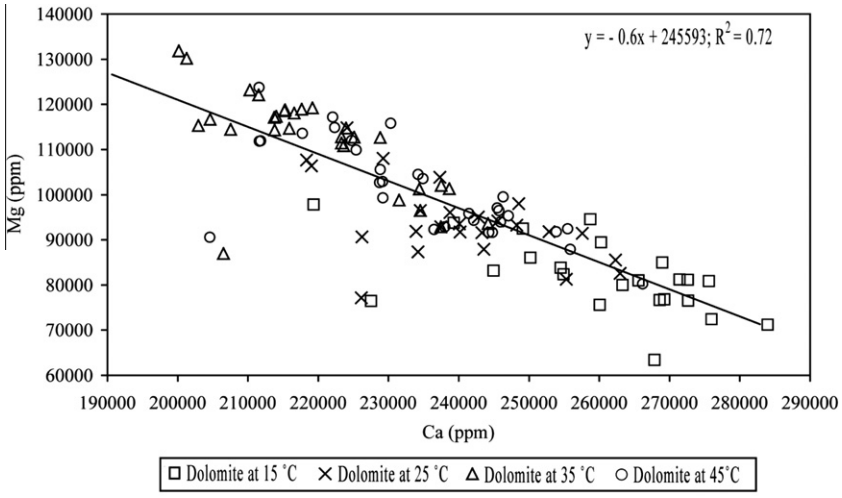

Fig. 3. Plot of Mg versus Ca concentrations of the dolomite precipitated in all cultures experiments at 15, 25, 35 and 45 °C.

show a systematic enrichment in Mg and Sr, with maximum values being reached at temperatures near the optimum bacteria activity (35–37 °C) and at 45 °C. The sum of the (Mg + Sr)/Ca molar ratios in the bacteria-medium interface ("bmi") are higher at 35 °C than at 15, 25 or 45 °C (see Tables 3 and 4; Fig. 2A). Also, both *V. marismortui* and *H. meridiana* concentrated Sr in the "bmi" up to 13.5 times higher than the original Sr concentration of the medium (20 ppm). The average Sr concentration in the "bmi" increased with temperature, from 80 ppm ± 0.1 ($n = 2$) at 15 °C to 149 ppm ± 0.20 ($n = 2$) at 45 °C in *V. marismortui* and *H. meridiana* cultures without sulfate and from 134 ppm ± 0.11 ($n = 2$) at 15 °C to 228 ppm ± 0.10 ($n = 2$) at 45 °C, Sr average values of both *V. marismortui* and *H. meridiana* cultures with sulfate (Table 4). We observe that when sulfate is present in the cultures, the Sr concentration in the "bmi" is higher than in cultures without sulfate (see Tables 3 and 4).

The Mg/Ca molar ratio of the dolomite varied with temperature from 0.52 ± 0.04 ($n = 2$) at 15 °C to 0.73 ± 0.04 ($n = 2$) at 45 °C (see Table 6 and Fig. 2B). At 35 °C (optimum temperature for bacteria growth), the Mg/Ca molar ratio of the dolomite is closest to 1.0, the stoichiometric value for dolomite. The enrichment in Mg apparently occurs at the expense of Ca substitution as expressed by a strong negative correlation between wt% Ca vs wt% Mg (Fig. 3). Also, Sr shows enrichment in the solid phase together with Mg as a function of increasing temperature (Tables 5 and 6; Fig. 2B). However, there is no indication that this occurs by Sr homogeneous substitution of Ca in the crystal lattice, as shown by the lack of any linear correlation between Sr and Ca (Fig. 4A and B). The weak correlation between Sr and Ca may suggest an adsorption process or occlusion instead of a paired exchange. Note in Fig. 4 that the Sr concentrations are relatively higher in dolomite produced in culture experiments with sulfate.

Fig. 5 illustrates the temperature dependence of the average value of Sr concentration in dolomite precipitated in both *V. marismortui* and *H. meridiana* cultures. Note that the Sr concentration in the dolomite increases with increasing temperature. In addition to the temperature variation, the Sr concentrations of the dolomite precipitated in cultures without sulfate range from 2877 ppm ± 0.11 ($n = 8$) at 15 °C to 3809 ppm ± 0.12 ($n = 8$) at 45 °C, whereas, in cultures with sulfate, they vary from 4012 ppm ± 0.20 ($n = 8$) at 15 °C to 6296 ppm ± 0.10 ($n = 8$) at 45 °C (see Table 5). As previously mentioned, *V. marismortui* and *H. meridiana* concentrate Sr in the "bmi", similar to the accumulation of Sr in the dolomite crystals, which is from 147 times at 15 °C to 190 times at 45 °C in cultures without sulfate and from 207 times at 15 °C to 313 times at 45 °C in cultures with sulfate. This large enrichment is relative to the original Sr concentration of 20 ppm in the medium.

3.3. Sr partition coefficient for dolomite, D_{Sr}^{dol}

The weak correlation between Sr and Ca concentration in the dolomite (Fig. 4A and B; $R^2 = 0.20$ and 0.36, respectively) appears to indicate that Sr does not homogeneously replace Ca in the crystal lattice. Thus, we propose that the

Table 5
Average Sr concentration and Mg/Ca, Sr/Ca and (Mg + Sr)/Ca molar ratios for dolomite from *V. marismortui* and *H. meridiana* cultures without and with sulfate.

T (°C)	Dolomite from *V. marismortui* cultures						Dolomite from *H. meridiana* cultures					
	Without sulfate			With sulfate			Without sulfate			Without sulfate		
	Sr (ppm)	Mg/Ca	Sr/Ca	(Mg + Sr)/Ca	Mg/Ca	Sr/Ca	(Mg + Sr)/Ca	Sr (ppm)	Mg/Ca	Sr/Ca	(Mg + Sr)/Ca	Sr (ppm)	Mg/Ca	Sr/Ca	(Mg + Sr)/Ca
15	2992 ± 0.12	0.50 ± 0.15	0.005 ± 0.13	0.51 ± 0.14	4012 ± 0.20	0.53 ± 0.09	0.007 ± 0.09	0.54 ± 0.21	2877 ± 0.11	0.56 ± 0.17	0.005 ± 0.19	0.57 ± 0.17	4290 ± 0.10	0.50 ± 0.07	0.008 ± 0.12	0.51 ± 0.07
25	3149 ± 0.16	0.65 ± 0.14	0.006 ± 0.18	0.66 ± 0.14	5164 ± 0.08	0.67 ± 0.15	0.010 ± 0.15	0.68 ± 0.12	2793 ± 0.17	0.65 ± 0.14	0.005 ± 0.28	0.66 ± 0.14	4904 ± 0.19	0.64 ± 0.12	0.009 ± 0.24	0.65 ± 0.12
35	3492 ± 0.12	0.82 ± 0.21	0.007 ± 0.16	0.83 ± 0.20	5565 ± 0.06	0.89 ± 0.10	0.012 ± 0.10	0.90 ± 0.07	3343 ± 0.10	0.80 ± 0.15	0.007 ± 0.15	0.81 ± 0.15	5563 ± 0.10	0.90 ± 0.04	0.012 ± 0.13	0.91 ± 0.04
45	3809 ± 0.12	0.75 ± 0.14	0.008 ± 0.15	0.76 ± 0.14	6296 ± 0.10	0.74 ± 0.14	0.012 ± 0.14	0.75 ± 0.14	3800 ± 0.02	0.71 ± 0.16	0.007 ± 0.06	0.72 ± 0.17	6211 ± 0.18	0.66 ± 0.15	0.012 ± 0.23	0.67 ± 0.15

Note: $n = 8$, average values calculated from Tables 2 and 3 in the Appendix.

Table 6
Average Sr concentration and Mg/Ca, Sr/Ca and (Mg + Sr)/Ca molar ratios for dolomite from both *V. marismortui* and *H. meridiana* culture experiments.

T (°C)	Dolomite from cultures without sulfate				Dolomite from cultures with sulfate			
	Sr (ppm)	Mg/Ca (M)	Sr/Ca (M)	(Mg + Sr)/Ca	Sr (ppm)	Mg/Ca(M)	Sr/Ca (M)	(Mg + Sr)/Ca
15	2935 ± 0.03	0.53 ± 0.08	0.005 ± 0	0.54 ± 0.08	4151 ± 0.05	0.52 ± 0.04	0.007 ± 0.09	0.52 ± 0.04
25	2971 ± 0.08	0.65 ± 0	0.006 ± 0.13	0.66 ± 0	5034 ± 0.04	0.66 ± 0.03	0.010 ± 0.07	0.66 ± 0.03
35	3418 ± 0.03	0.81 ± 0.02	0.007 ± 0	0.82 ± 0.02	5564 ± 0	0.90 ± 0.01	0.012 ± 0	0.91 ± 0.01
45	3805 ± 0.02	0.73 ± 0.04	0.008 ± 0.09	0.74 ± 0.04	6254 ± 0.01	0.70 ± 0.08	0.012 ± 0	0.71 ± 0.08

Note: $n = 2$, average values calculated from Table 5.

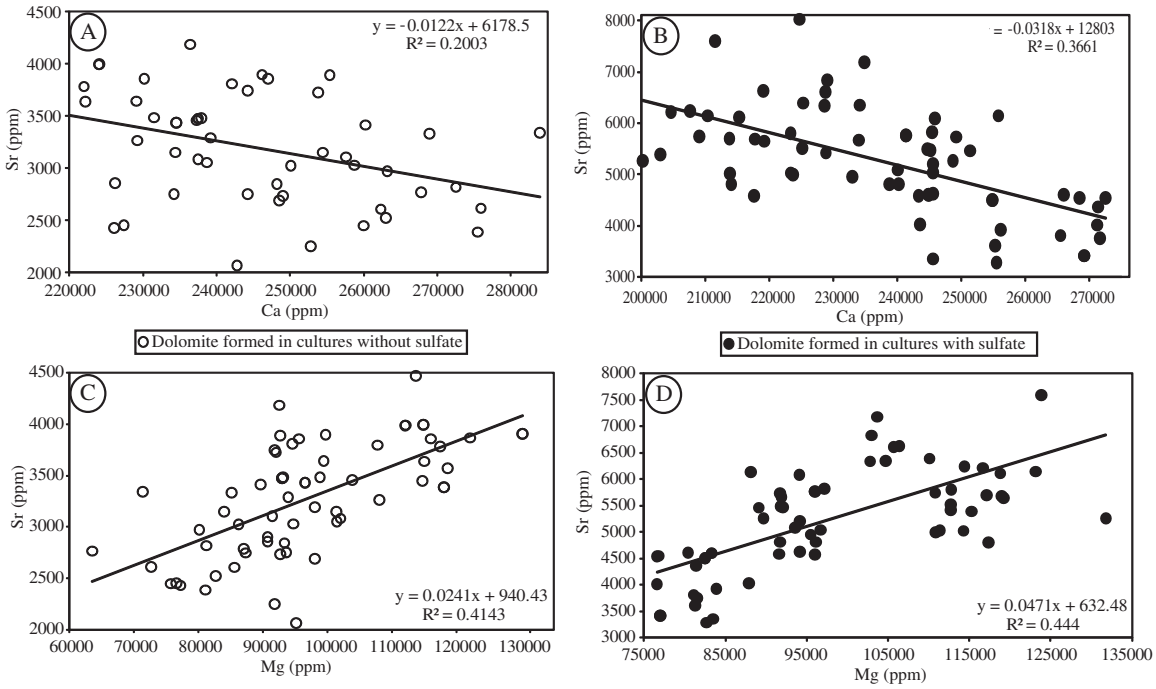

Fig. 4. Plots of Sr versus Ca (A and B) and of Sr vs Mg (C and D) concentrations of the dolomites precipitated in culture experiments with and without sulfate, as indicated by closed and open circles, respectively.

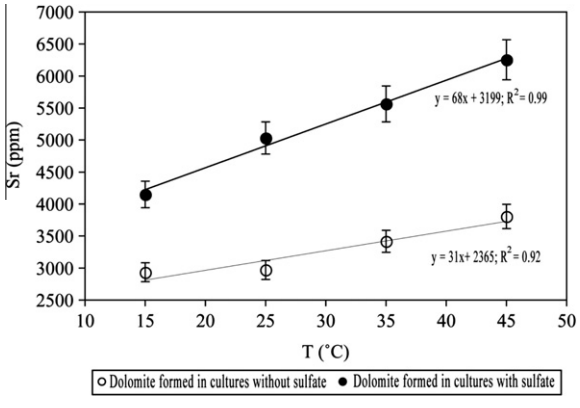

Fig. 5. Average values of Sr concentrations in dolomite precipitates versus temperature in cultures with and without sulfate, as indicated by the closed and open circles, respectively.

Sr enrichment mechanism is most probably related to surface adsorption or occlusion on the dolomite crystal. The partition coefficient for Sr in the solid phase is best represented for our experimental data by the molar ratio of the concentration in the solid phase (dolomite, "dol") over that in the fluid ("bmi"), which is expressed as $D_{Sr}^{dol} = Sr_{dol}/Sr_{bmi}$ using the Nernst partition coefficient (1891). However, all previous studies have defined the Sr partition coefficient for natural dolomites (Baker and Burns, 1985; Vahrenkamp and Swart, 1990) and recrystallization of dolomite (Malone et al., 1994, 1996) using the equation of Henderson and Kracek (1927), where D_{Sr}^{dol} is the homogeneous partition coefficient for the homogeneous incorporation of Sr in dolomite. These authors assume that: (1) Sr/Ca of the solid (dolomite) and Sr/Ca ratio of the solution from which dolomite precipitates are in equilibrium and (2) Sr homogeneously replaces Ca in the crystal lattice. This is in accordance with the definition of homogeneous solid solution formation, that is, in an ideal system the ratio of the solubility products of the major and trace element carbonates define the partitioning coefficient. Therefore, the partition factor given as $D_{Sr}^{dol} = (Sr/Ca)_{dol}/(Sr/Ca)_{fluid}$, using the equation of Henderson and Kracek (1927), may not be applicable to the present study because there is no empirical evidence of homogeneous distribution of the impurity. The Nernst equation seems more adequate to describe the

partition between the medium and the solid phase in our system, since it does not presume a specific partition model.

Because our results are achieved using bacteria culture experiments, which represent a new untested approach to determine the Sr partition coefficient for dolomite, whereas previous studies utilize natural geologic samples and modeled environmental conditions, we chose to calculate the Sr partition coefficient for dolomite (D_{Sr}^{dol}) using both the Nernst and Henderson and Kracek equations for comparative purposes. The calculated D_{Sr}^{dol} values formed in both *V. marismortui* and *H. meridiana* cultures are reported in Tables 7 and 8, respectively. As both bacterial species have the optimal growth at 35–37 °C and similarly incorporate Sr into dolomite, we have represented the biomediated partition coefficient for dolomite as the average D_{Sr}^{dol} values calculated for the dolomite formed in *V. marismortui* and *H. merididana* cultures with and without sulfate, respectively (Table 9).

The averaged D_{Sr}^{dol} values based on calculations using both the Nernst and Henderson and Kracek equations are plotted versus temperature in Fig. 6. Based on our interpretation of the results, we must assume that the partitioning of Sr between the solid and "bmi" phases is not in homogeneous equilibrium, and the Nernst equation would best define D_{Sr}^{dol}. In Fig. 6A, we observe that the correlation between the D_{Sr}^{dol} and temperature is a second order polynomial, and the maximum D_{Sr}^{dol} values are 31 ± 0.15 ($n = 2$) and 37 ± 0.01 ($n = 2$) at 15 °C in cultures with sulfate and without sulfate, respectively. The minimum values ($D_{Sr}^{dol} = 21$ and 22) occur at 35 °C, where the bacteria have their maximum growth. Also, in contrast to the experiments at 15 °C, we observe that, at 25, 35 and 45 °C, D_{Sr}^{dol} values are greater in cultures with sulfate than in cultures without sulfate.

On the other hand, if we were to assume homogeneous equilibrium conditions for our experiments, we could define D_{Sr}^{dol} with the Henderson and Kracek equation. In Fig. 6B, we observe that the correlation between the D_{Sr}^{dol} and temperature is linear and the maximum D_{Sr}^{dol} values are 0.23 ± 0.03 ($n = 2$) and 0.15 ± 0.04 ($n = 2$) at 45 °C in cultures with sulfate and without sulfate, respectively. Also, D_{Sr}^{dol} values are significantly greater in cultures with sulfate than in cultures without sulfate and with increasing temperature.

Using the Nernst equation, we obtain the minimum D_{Sr}^{dol} values at 35 °C, because at 35 °C the bacteria have their maximum growth producing a greater availability of ions (Sr, Ca, Mg) in the interface medium bacteria ("bmi", site of mineral precipitation) than at lower or higher temperatures. However, using Henderson and Kracek equation the maximum D_{Sr}^{dol} values occur at 35 and 45 °C, where the maximum Sr incorporation occurs. Because the D_{Sr}^{dol} defined with the Nernst equation reflects the temperature effect on microbial activity, we propose that the Nernst equation is most appropriate to define $D_{Sr}^{dol.}$.

4. DISCUSSION

4.1. Sr-content of natural and ancient dolomites

There is evidence that some ancient and modern dolomite formation is related to microbial activity (Baker and Burns, 1985; Vasconcelos and McKenzie, 1997; Wright, 1999; Garcia del Cura et al., 2001; van Lith et al., 2003a; Roberts et al., 2004; Moreira et al., 2004; Wright and Wacey, 2005; Mastandrea et al., 2006; Sánchez-Román et al., 2008, 2009a). Microbial dolomite from culture experiments has been found to be closely associated with bacteria (van Lith et al., 2003b; Warthmann et al., 2000; Sánchez-Román et al., 2008, 2009b). Indeed, Sánchez-Román et al. (2009b) hypothesized that the formation of dolomite in natural environments, depleted or enriched in sulfate, is associated with the degradation of organic matter by moderately halophilic aerobic bacteria (MHAB) and, specially, by the production of ammonia which is vital to dolomite formation. In fact, nearly all dolomite forming in marine and/or lacustrine environments, develops in sediments rich in organic matter (Baker and Burns, 1985; De Deckker, 1988; Rosen et al., 1988; Vasconcelos and McKenzie, 1997; Meister et al., 2007; Sánchez-Román et al., 2009b). Thus, for this study, a gel-medium with seawater NaCl concentration and enriched in amino acids (carbon source for the bacteria), as well as Ca, Mg and Sr, was prepared. The experiments were designed to test and to understand Sr co-precipitation in dolomite.

The Sr concentrations found in the dolomites formed in aerobic culture experiments are an order of magnitude higher than those reported for most ancient dolomites, e.g., the cap dolostone from the Neoproterozoic which have an average value for Sr of less than 100 ppm (James et al., 2001; Hurtgen et al., 2006). However, there are some exceptions, such as the dolomite of the Oligocene Tikorangi Formation in New Zealand and the Permian saline lakes in Western Pyrenees which have average Sr concentrations of 3300 and 2230 ppm, respectively (values extrapolated from Valero and Gisbert, 1994; Hood et al., 2004). In addition, the dolomite found in most Holocene-Pleistocene environments is characterized by a high content of Sr (Behrens and Land, 1972; Land, 1973; Land and Hoops, 1973; Müller and Wagner, 1978; Botz and von der Borch, 1984; Baker and Burns, 1985; Humphrey, 1988; Banner et al., 1991; Mazzullo et al., 1995). We note that the dolomite forming in the Coorong area (South Australia) and in the Falmouth Formation (North Jamaica) are extremely rich in Sr with average values of 7000 and 3000 ppm, respectively (values extrapolated from Land, 1973; Botz and von der Borch, 1984). The Sr values of these dolomite examples are in the range of our experimentally produced microbial dolomite, which have Sr average values ranging from 2877 to 6296 ppm. A possible explanation for these high Sr^{2+} concentrations in natural and experimental dolomite is bacterial origin.

4.2. Influence of bacterial metabolism on Sr co-precipitation with dolomite

The ability of bacterial cells to bind metal ions, such as Ca, Mg and Sr, to the functional groups of their cell walls is well known (Faison et al., 1990; Friis et al., 2003). Bacteria have the capacity to adsorb ions, mainly Ca and Mg, on their cell envelope, creating micro-environments which induce the precipitation of minerals. This process does

Table 7
Sr partition coefficient for dolomite (D_{Sr}^{dol}) from *V. marismortui* cultures at 15, 25, 35 and 45 °C.

T (°C)	Cultures without sulfate						Cultures with sulfate					
	Sr_{dol} (ppm)	Sr_{bmi} (ppm)	$^1D_{Sr}^{dol}$	$(Sr/Ca)_{dol}$	$(Sr/Ca)_{bmi}$	$^2D_{Sr}^{dol}$	Sr_{dol} (ppm)	Sr_{bmi} (ppm)	$^1D_{Sr}^{dol}$	$(Sr/Ca)_{dol}$	$(Sr/Ca)_{bmi}$	$^2D_{Sr}^{dol}$
15	2992 ± 0.12	86 ± 0.07	35 ± 0.12	0.0051 ± 0.13	0.044 ± 0.44	0.12 ± 0.13	4012 ± 0.20	145 ± 0.20	28 ± 0.2	0.0071 ± 0.09	0.036 ± 0.33	0.20 ± 0.21
25	3149 ± 0.16	160 ± 0.10	20 ± 0.17	0.0060 ± 0.18	0.046 ± 0.21	0.13 ± 0.18	5164 ± 0.08	207 ± 0.03	25 ± 0.08	0.0100 ± 0.15	0.045 ± 0.15	0.22 ± 0.11
35	3492 ± 0.12	156 ± 0.23	22 ± 0.12	0.0073 ± 0.16	0.051 ± 0.29	0.14 ± 0.16	5565 ± 0.06	250 ± 0.09	22 ± 0.06	0.0117 ± 0.10	0.054 ± 0.21	0.22 ± 0.07
45	3809 ± 0.12	171 ± 0.03	22 ± 0.12	0.0078 ± 0.15	0.051 ± 0.19	0.15 ± 0.15	6296 ± 0.10	245 ± 0.04	26 ± 0.1	0.0124 ± 0.14	0.054 ± 0.05	0.23 ± 0.14

Note: $n = 8$, average values calculated from Table 2 in the Appendix.
$^1D_{Sr}^{dol}$ defined with Nernst equation; $^2D_{Sr}^{dol}$ defined with Henderson and Kracek equation.

Table 8
Sr partition coefficient for dolomite (D_{Sr}^{dol}) from *H. meridiana* cultures at 15, 25, 35 and 45 °C.

T (°C)	Cultures without sulfate						Cultures with sulfate					
	Sr_{dol} (ppm)	Sr_{bmi} (ppm)	$^1D_{Sr}^{dol}$	$(Sr/Ca)_{dol}$	$(Sr/Ca)_{bmi}$	$^2D_{Sr}^{dol}$	Sr_{dol} (ppm)	Sr_{bmi} (ppm)	$^1D_{Sr}^{dol}$	$(Sr/Ca)_{dol}$	$(Sr/Ca)_{bmi}$	$^2D_{Sr}^{dol}$
15	2877 ± 0.11	74 ± 0.07	38.8 ± 0.11	0.0053 ± 0.19	0.036 ± 0.07	0.15 ± 0.19	4290 ± 0.10	123 ± 0.04	35 ± 0.10	0.0075 ± 0.12	0.038 ± 0.14	0.20 ± 0.12
25	2793 ± 0.17	85 ± 0.17	33 ± 0.21	0.0054 ± 0.28	0.045 ± 0.05	0.12 ± 0.28	4904 ± 0.19	165 ± 0.09	30 ± 0.19	0.0094 ± 0.24	0.045 ± 0.02	0.21 ± 0.24
35	3343 ± 0.10	162 ± 0.28	21 ± 0.1	0.0068 ± 0.15	0.048 ± 0.12	0.14 ± 0.12	5563 ± 0.10	252 ± 0.04	22 ± 0.18	0.012 ± 0.13	0.055 ± 0.06	0.22 ± 0.13
45	3800 ± 0.02	127 ± 0.16	30 ± 0.02	0.0072 ± 0.17	0.051 ± 0.07	0.14 ± 0.06	6211 ± 0.18	211 ± 0.08	29 ± 0.18	0.0118 ± 0.23	0.053 ± 0.12	0.22 ± 0.23

Note: $n = 8$, average values calculated from Table 3 in the Appendix.
$^1D_{Sr}^{dol}$ defined with Nernst equation; $^2D_{Sr}^{dol}$ defined with Henderson and Kracek equation.

Table 9
Average D_{Sr}^{dol} values for both *V. marismortui* and *H. meridiana* cultures without and with sulfate at 15°, 25°, 35° and 45 °C.

T (°C)	Cultures without sulfate					Cultures with sulfate				
	Sr_{dol} (ppm)	Sr_{bmi} (ppm)	$^1D_{Sr}^{dol}$	$(Sr/Ca)_{dol}$	$(Sr/Ca)_{bmi}$	$^2D_{Sr}^{dol}$	Sr_{dol} (ppm)	Sr_{bmi} (ppm)	$^1D_{Sr}^{dol}$	$(Sr/Ca)_{dol}$	$(Sr/Ca)_{bmi}$	$^2D_{Sr}^{dol}$
15	2935 ± 0.03	80 ± 0.1	37 ± 0.01	0.0052 ± 0	0.0400 ± 0.14	0.13 ± 0.15	4151 ± 0.05	134 ± 0.11	31 ± 0.15	0.0073 ± 0.09	0.0370 ± 0.03	0.20 ± 0
25	2971 ± 0.08	123 ± 0.43	24 ± 0.35	0.0057 ± 0.13	0.0455 ± 0.01	0.13 ± 0.05	5034 ± 0.04	186 ± 0.15	27 ± 0.12	0.0097 ± 0.07	0.0450 ± 0	0.22 ± 0.03
35	3418 ± 0.03	159 ± 0.02	21.5 ± 0.03	0.0071 ± 0	0.0495 ± 0.04	0.14 ± 0	5564 ± 0	251 ± 0.05	22 ± 0	0.0119 ± 0	0.0545 ± 0.01	0.22 ± 0
45	3805 ± 0.002	149 ± 0.20	25.5 ± 0.21	0.0075 ± 0.09	0.0510 ± 0	0.15 ± 0.04	6254 ± 0.01	228 ± 0.10	27.5 ± 0.07	0.0121 ± 0	0.0535 ± 0.01	0.23 ± 0.03

Note: $n = 2$, average values calculated from Tables 7 and 8.
$^1D_{Sr}^{dol}$ defined with Nernst equation; $^2D_{Sr}^{dol}$ defined with Henderson and Kracek equation.

not occur in the absence of bacterial activity (e.g., Sánchez-Román et al., 2007, 2008, 2009a,b). Thus, bacteria can act as a nucleus for mineral precipitation by absorbing cations around the cellular surface membrane or cell wall (Morita, 1980; Ferris et al., 1991; Braissant et al., 2003; Sánchez-Román et al., 2008). According to previous studies, *V. marismortui* and *H. meridiana* would be able to adsorb and bind Ca, Mg and Sr to the functional groups of their cell walls.

Our experiments demonstrate that it is possible to produce dolomite at Earth surface temperatures (15, 25, 35 and 45 °C) in the laboratory under oxic, (hyper)saline conditions with or without sulfate ions in the presence of MHAB. During the bacterial growth experiments using a gel-medium rich in organic matter (peptone and yeast extract as sources for CO_2 and NH_3), the pH and carbonate concentration increased because of the production of CO_2 and NH_3 (which hydrate to form CO_3^{2-} and NH_4^+, respectively) during metabolization of organic nutrients, according to the following equation:

$$C_{106}H_{263}O_{110}N_{16}P_1 + 107O_2 + 14H^+ \rightarrow 106CO_2 + 16NH_4^+ + HPO_4^{2-} + 108H_2O \quad (1)$$

(Stumm and Morgan, 1996).

These changes, together with the adsorption of Mg and Ca ions by *V. marismortui* and *H. meridiana*, would drive local supersaturation gradients and induce precipitation of dolomite around bacteria surfaces, using these as nucleation sites.

It is important to understand how super-saturation develops in the gel medium. In abiotic medium, no formation of precipitates is observed, firstly, because carbonate ions are not generated and, secondly, because most probably all Ca, Mg, and Sr ions are strongly bound to the ligand groups in the amino acids, containing oxygen and nitrogen atoms as electron donors. When the gel is formed and water molecules are bound to the colloidal particles, these ions are immobilized in the amino acid array and can only be liberated by significantly changing the physical and chemical conditions. Such changes do, however, occur in the presence of bacteria, which by metabolizing the organic substances liberate CO_2, NH_3, H_2O, HPO_3^{2-}, Ca^{2+}, Mg^{2+} and Sr^{2+}. Molecular diffusion in this medium is too slow to allow significant bacteria growth rates. Therefore, liberation of Ca^{2+}, Mg^{2+} and Sr^{2+} must be associated with the uptake of the organic matter. The presence of "free" water is essential for hydration of CO_2 and protonation of ammonia (NH_3) that leads to an alkaline pH. Under these conditions, high pH and availability of inorganic carbon, carbonate ions can be formed in the bacteria-medium interface (bmi). The agar medium slows the diffusion of ions away from the interface, which, as the bacteria growth proceeds, becomes progressively enriched in the ions of interest (Ca^{2+}, Mg^{2+}, Sr^{2+} and CO_3^{2-}) until supersaturation is reached. Because precipitation of dolomite in the water phase is not observed, the set of conditions, established by the biological metabolism, combine to weaken diffusion of ion away from the source and apparently are essential for precipitation of dolomite. Thus, the activity at the bacteria

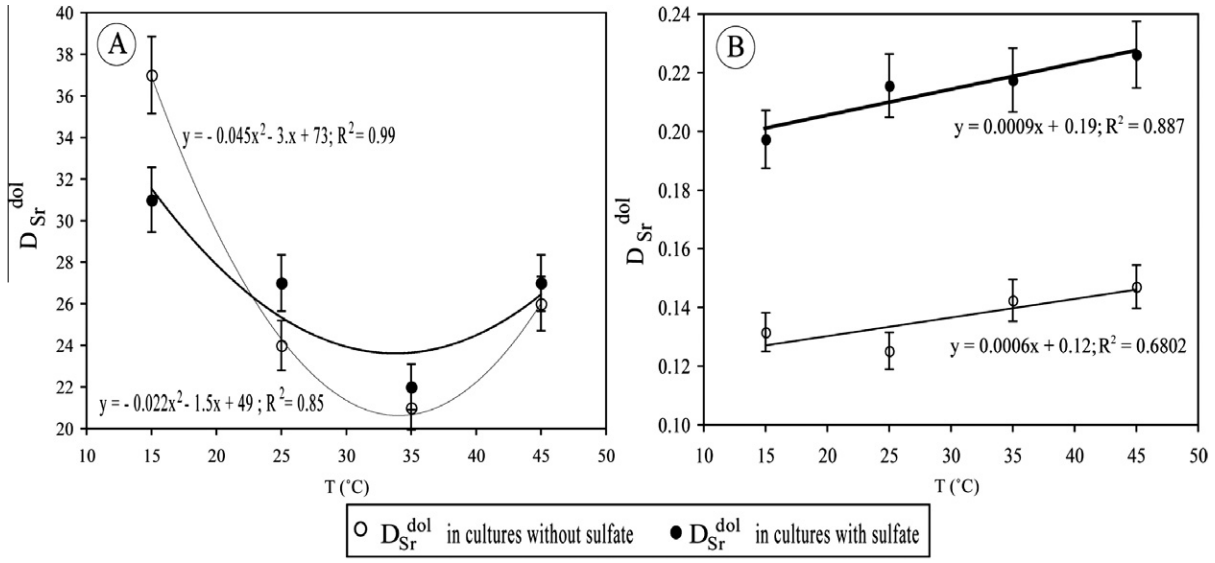

Fig. 6. Average values of the biomediated Sr partition coefficient (D_{Sr}^{dol}) in cultures with and without sulfate at 15, 25, 35 and 45 °C. (A) D_{Sr}^{dol} definedwith Nernst equation (1891) and (B) D_{Sr}^{dol} defined with Henderson and Kracek equation (1927).

surface tends to lower the activation energy required for nucleation of dolomite as well as promoting the availability of cations.

The maximum enrichment of Mg and Sr in the "bmi" and in the dolomite crystals occurs at 35 °C (Fig. 2), most probably due to the fact that 35–37 °C is the optimal growth temperature range for the bacteria investigated. Thus, at this temperature range, the bacteria have the maximum metabolic activity, being capable of metabolizing more efficiently nutrients from the medium than at lower temperatures. Therefore, at higher temperatures more ions (Ca, Mg, and Sr) will be liberated in the "bmi" by the bacteria, creating most suitable conditions for stoichiometric dolomite formation. As observed in Table 6, dolomite formed at 35 °C (optimal bacteria growth) has a Mg/Ca molar ratio between 0.81 ± 0.02 ($n = 2$) and 0.90 ± 0.01 ($n = 2$) approaching the stoichiometric ratio.

On the other hand, the higher average values of Sr in dolomite are found at the higher experimental temperatures used in this study (Table 9; Fig. 5). This relationship has also been demonstrated for metals (Sr, Mn, Fe and Mg) in studies of calcite precipitation rates (Katz et al., 1972; Katz, 1973; Dromgoole and Walter, 1990). Such behaviour is common in geochemical systems, where miscibility of ions in minerals increases with increasing temperature (Stumm and Morgan, 1996). We have demonstrated that the incorporation of metals into dolomite is not only a function of temperature and/or precipitation rate but, also, bacteria metabolic activity and sulfate concentration. Furthermore, we have demonstrated that all these parameters together not only affect the mineral composition but, also, the medium composition at the site of mineral precipitation. The molar ratios of Mg/Ca and Sr/Ca in the "bmi" of cultures with sulfate were greater than in the "bmi" of cultures without sulfate. Therefore, the dolomite precipitated from cultures with sulfate has more Sr incorporated than the dolomite precipitated from cultures without sulfate (Table 9 and Fig. 5). This observation is consistent with the fact that most natural Sr-rich dolomite have formed in environments containing relatively high sulfate concentrations (Behrens and Land, 1973; Land, 1973; Videtich, 1982; Botz and von der Borch, 1984; Humphrey, 1988; Valero and Gisbert, 1994).

Our experimental results show that high Sr compositions in ancient and Recent dolomites could reflect microbial mediation. Previously, high Sr concentrations in natural dolomites have been interpreted as an indicator of secondary replacement after aragonite, which incorporates high Sr concentrations in its crystal lattice, reflecting a diagenetic process (Land, 1973; Bein and Land, 1983; Humphrey, 1988). However, our Sr data clearly show that primary dolomite can have high contents of Sr, as high or higher than those commonly measured for aragonite. Thus, Sr-rich dolomite found in nature (Botz and von der Borch, 1984; Land, 1973; amongst many others) probably formed as a primary precipitated in association with bacteria and not necessarily by secondary replacement of aragonite. In addition, modern dolomite often seems to have formed under the oxidizing conditions characteristic of shallow-water carbonate shelves and are Sr-rich compared to most ancient dolomite (Land, 1985). This observation is consistent with our microbial dolomite produced in aerobic culture experiments, which has a high content of Sr. Thus, most natural Sr-rich dolomites may be primary precipitates mediated by aerobic microbial activity. We tentatively conclude that a high Sr composition in ancient and recent dolomites may be an indicator of primary dolomite precipitation induced by bacteria under aerobic conditions. In fact, most Recent Sr-rich dolomite is associated with organic matter (Behrens and Land, 1972; Botz and von der Borch, 1984; Mazzullo et al., 1995), and there is evidence that some ancient Sr-rich dolomites formed in organic-rich lacustrine environments (Valero and Gisbert, 1994; Garcia del Cura et al., 2001).

4.3. Implications of biomediated partition coefficient (D_{Sr}^{dol}) using Nernst equation

Many authors have used trace elements to elucidate the origin of dolomite. In general, the trace element content of a crystal is proportional to the trace element content of the solution from which the crystal forms. This fractionation between a solid and solution is represented by a constant, D, which is called a partition coefficient.

Trace metals may be incorporated into minerals via (1) impurities such as fluid or mineral inclusions, (2) occlusion in lattice defects, (3) sorption onto growing crystal surfaces and (4) solid solution formation by substitution for a major element that is an essential structural constituent (i.e., a lattice component) of the mineral (McIntire, 1963; Sun and Hanson, 1975). Theoretical and experimental approaches to modeling the trace element behavior of Sr in dolomite-fluid systems assume that a solid-solution substitution of Sr into Ca structural sites is the only significant mechanism (Behrens and Land, 1972; Katz and Mathews, 1977; Kretz, 1982; Baker and Burns, 1985; Vahrenkamp and Swart, 1990; amongst others). However, our results show that there is a strong inverse correlation between Mg and Ca concentration in the obtained solids suggesting an on-going homogeneous replacement while such a relation is very weak in the case of Sr, which can be present in the crystal as an adsorbed or occluded impurity entering the system as the growth proceeds (Figs. 3 and 4A, B). Also, for calcite it has been stated that there is no agreement about whether Sr cations substitute for Ca in the crystal lattice (Reeder et al., 1999, 2002). Additionally, a compilation of published Sr and Ca data from seven dolomite occurrences indicates a similar lack of correlation between the Sr and Ca concentrations, even though they are from different locations and of vastly different ages (Fig. 7). The published data are consistent with our results in that Sr does not apparently replace Ca homogeneously in the crystal lattice. Thus, we propose that the Sr enrichment in our experimental and the reported natural dolomite is most probably related to surface adsorption or occlusion and not by solid solution substitution. This assumption is in agreement with the following considerations related to the crystal chemistry of Ca–Mg–Sr carbonates.

Crystal chemical substitution of Ca for Mg in rhombohedral carbonates produces a well-known lattice contraction (specifically an anion sub-lattice contraction) because of Mg–O distances are shorter than Ca–O distances. In this sense, the incorporation of Mg instead of Ca to the carbonate rhombohedral structure would drastically reduce the available space in the metal site; which precludes the incorporation of large cations such as Sr into the small interstices between the anions of the contracted rhombohedral structure. The substitution of Sr for Ca commonly occurs in the aragonite structure, which is isostructural with the strontianite structure, because the Ca has higher coordination (larger ionic radii) in the aragonite structure than in the

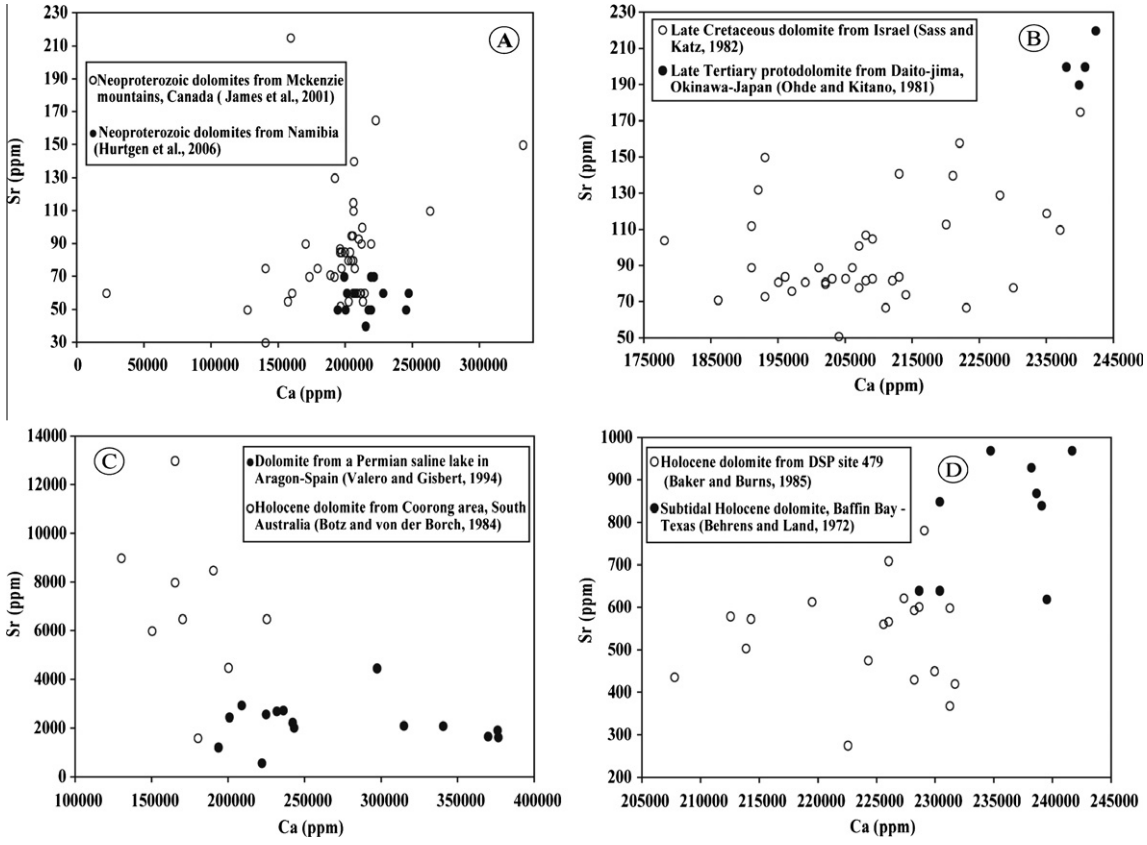

Fig. 7. Sr versus Ca contents of some ancient and recent dolomites.

calcite structure. Therefore, Sr should be incorporated in rhombohedral carbonates via occlusion in lattice defects or sorption onto crystal (nano-crystal) surfaces. Our data indicate that dolomites are richer in Sr as Ca is substituted by Mg in the structure, the incorporation of Mg apparently favours the incorporation of Sr in the dolomite lattice (Figs. 3 and 4C, D). To explain how the crystal chemical substitution of Mg for Ca within the structure of rhombohedral carbonates favours the Sr sorption, we must deal with nonbonded repulsion between CO_3^{2-} anions within the structure. Such repulsion increases as the anion sub-lattice contracts and the distance between CO_3^{2-} anions decreases because of the Mg incorporation into the structure. It is known that nonbonded repulsion (also called "Pauli repulsions") removes electron density from regions of low-potential energy, and concentrates electrons at the antibinding regions, where the electrons feel less the potential of the nucleii (Bader and Preston, 1966; Bader, 2006). Hence, the increase of nonbonded repulsion between CO_3^{2-} anions makes the valence electrons feel less the oxygen potential well within the CO_3^{2-} anions. The decrease of the electron binding energy in the O atoms increases the oxygen polarizability. The improvement of the so-called polarization, correlation or Van der Waals forces between CO_3^{2-} anions and Sr^{2+} cations (with higher polarizability, 1.4, arbitrary units than Ca^{2+}, 0.6, or Mg^{2+}, 0.1), explains the incorporation of Sr at the dolomite crystal surface.

Based on the above interpretation, the Sr partition coefficient for dolomite (D_{Sr}^{dol}) is represented here by the Nernst equation, the Sr ratio of the concentration in dolomite over the concentration in the "bmi". Thus, the D_{Sr}^{dol} is a function of the medium composition. We have demonstrated that the Sr concentration of the "bmi" (site of dolomite precipitation) and dolomite are dependent on microbial activity and temperature. Therefore, D_{Sr}^{dol} will be affected by the bacterial metabolic activity. The values of D_{Sr}^{dol} at 15 and 25 °C are lower than at 35 and 45 °C. In particular, at 35 °C, D_{Sr}^{dol} has the lowest value because the bacteria liberate more Sr at the optimal growth temperature (35–37 °C). Thus, the concentration of Sr in the "bmi" (site of dolomite precipitation) will be greater than in experiments run at lower (15 and 25 °C) or higher temperature (45 °C). D_{Sr}^{dol} at 45 °C is slightly higher than at 35 °C because at high temperatures the miscibility of ions in minerals increases (Stumm and Morgan, 1996). Therefore, more Sr will be incorporated into dolomite at 45 °C than at 35 °C. See Fig. 6 and Table 9.

Using our derived D_{Sr}^{dol} from experiments with sulfate based on the Nernst equation, we can calculate the Sr composition of ancient dolomite solutions corresponding to the Sr composition of the dolomite. Application of our findings to published Sr data for natural dolomite with different ages and from different locations provides new paleoenvironmental information for the following two different environments: (1) Carbonate platform dolomite: (a) late Tertiary Daijito-jima dolomite, in Japan, precipitated from fluids with a Sr concentration similar to modern seawater (8 ppm) (Fig. 7B and Table 10), whereas (b) Late Cretaceous dolomite, in Israel, seems to have formed in water with lower Sr concentrations (~4 ppm) than seawater concentration (Fig. 7B and Table 10). (c) Neoproterozoic Cap-dolostones, Mackenzie Mountains, Canada and in Namibia, also, show a lower than seawater Sr value (~2 ppm), (Fig. 7A and Table 10), indicating a salinity lower than seawater. The calculated Sr value is in accordance with the proposal that the post-Marinoan surface ocean was brackish, because, during the deglaciation, a mixed surface layer of brackish and oxic water dominated (Hurtgen et al., 2006). Furthermore, this mixed surface layer, from which the cap dolostones precipitated, had very low sulfate concentrations (Hurtgen et al., 2006). (2) Lacustrine dolomite: (a) Holocene dolomites from Coorong area and Baffin Bay, Texas, formed in waters with approximately 226 and 30 ppm Sr, respectively (Fig. 7C and D; Table 10). (b) Dolomite from a Permian lake, in Spain, formed from solutions with 88 ppm of Sr. Thus, modern and ancient lacustrine dolomite precipitated from fluids with Sr concentrations higher than modern seawater (8 ppm), indicating salinity greater than seawater. Furthermore, these lacustrine dolomite environments are hypersaline, enriched in sulfate and probably fed by groundwater high in Sr related to weathering of rocks in the catchment area. In addition, hypersaline and/or saline waters, apparently, are relatively rich in Sr with considerable sulfate concentration, whereas brackish waters are relatively poor in Sr and sulfate. Our findings suggest that lacustrine waters precipitating dolomite are the richest in Sr and sulfate. Indeed, the greatest Sr for natural dolomite are found in such lacustrine environments (Behrens and Land, 1972; Land, 1973; Botz and von der Borch, 1984; amongst others). We propose that

Table 10
Application of the biomediated Sr partition coefficients, using Nernst equation, for sedimentary dolomite. Sr concentrations in ppm.

Location/Age	Sr_{dol}	$^{d}D_{Sr}^{dol(sulfate)}$	T (°C)	$^{b}Sr_{water}^{(calculated)}$
[1]Daijito-Jima, Japan/Late Tertiary	203	27	25	7.5
[2]Israel/Late Cretaceous	97	27	25	3.6
[3]Namibia/Neoproterozoic	57	31	15	1.8
[4]McKenzie Mountains, Canada/Neoproterozoic	85	31	15	2.7
[5]Coorong, South Australia/Holocene	7010	31	15	226
[6]Baffin Bay, Texas/Holocene	814	27	25	30
[7]Aragon-Bearn Basin, Spain/Permian	2231	27	25	83

Notes: Sr-data of sedimentary dolomite extrapolated from: (1) Ohde and Kitano, 1981; (2) Sass and Katz (1982); (3) Hurtgen et al. (2006); (4) James et al. (2001); (5) Botz and von der Borch (1984); (6) Behrens and Land (1972); (7) Valero and Gisbert (1994).

Table 11
Recalculation of Sr, in ppm, for sedimentary dolomite and associated solutions.

Location/Age	Sr_{water}	Sr_{dol}	D_{sr}^{dol} @ 15 °C		D_{sr}^{dol} @ 25 °C	
			Sr_{dol} (calculated)	Sr_{water} (calculated)	Sr_{dol} (calculated)	Sr_{water} (calculated)
Brejo do Espinho/Holocene	935[a]	24[a]	744	30	648	34
DSDP Site 479/Plesitocene	535[b]	21[b]	651	17	567	22
Bahamas Bank/Late Tertiary	190[c]	8[c]	248	6	216	8

$Sr_{dol} = 190$ is a mean value extrapolated from Vahrenkamp and Swart (1990).
[a] Values extrapolated from Moreira et al. (2004).
[b] Mean values for Sr in dolomite and precipitating waters extrapolated from Baker and Burns (1985).
[c] We have assumed that these dolomites precipitated from solutions with same Sr composition as modern seawater (Sr = 8 ppm) as previously Vahrenkamp and Swart (1990) suggested.

Sr can be used as an indicator of paleosalinity and paleotemperature.

To further verify the applicability of the biomediated D_{Sr}^{dol}, we used published data of Sr concentrations of sedimentary dolomite and associated solution to recalculate the Sr values of the dolomite and associated solution. Using the D_{Sr}^{dol} value determined at 15 and 25 °C in the presence of sulfate (Table 11), we have reproduced the following: (1) Brejo do Espinho dolomite should have Sr concentrations of 744–648 ppm and the precipitating water 30–34 ppm of Sr, respectively, (2) Pleistocene dolomites from DSDP Site 479, in the Gulf of California, should have 651–567 ppm of Sr and the precipitating water should have 17–22 ppm of Sr, and, (3) the Sr concentration of the Late Tertiary dolomites from Bahamas Bank should be 248–216 ppm and should have formed from waters containing 6–8 ppm of Sr. We should note that we have assumed that both dolomites from DSDP Site 479 and the Bahamas have formed at ~15–25 °C and that the dolomite from Brejo do Espinho, Brazil, formed at ~21 °C (Sánchez-Román et al., 2009a).

The calculated Sr values obtained for these three natural dolomites and associated waters, using our biomediated D_{Sr}^{dol} at 15 and 25 °C in the present of sulfate, are nearly the same as the previously reported values (Baker and Burns, 1985; Vahrenkamp and Swart, 1990; Moreira et al., 2004; see Table 11). Thus, we have clearly demonstrated the applicability of the new D_{Sr}^{dol} which potentially can be used as an indicator of paleosalinity and paleotemperature to constrain ancient dolomitic environments.

In summary, ancient dolomite commonly has significantly low Sr concentrations (20–70 ppm) than would be expected from published Sr partition coefficient values (Baker and Burns, 1985; Vahrenkamp and Swart, 1990; amongst others) and Sr/Ca ratios of most modern sedimentary pore waters. However, our experimental D_{Sr}^{dol} values, defined with the Nernst equation, are consistent with Sr concentrations of ancient dolomites, Recent dolomites and associated solutions. Probably, the discrepancy associated with previous D_{Sr}^{dol} (Baker and Burns, 1985; Vahrenkamp and Swart, 1990; amongst others) and Sr content in ancient dolomites is due to the fact that these authors assumed that dolomite formed in a homogeneous solid solution, which implies homogeneous equilibrium and the replacement of Ca by Sr. Although, previous partition coefficients for dolomite show reasonable calculations for the estimation of Sr/Ca concentration in solution, we would like to point out that the experimental conditions in the laboratory culture experiments are controlled and do not represent the real world. Thus, we need to compare the experimentally biomediated Sr partition coefficient for dolomite with previous studies to better understand the natural conditions.

5. CONCLUSIONS

Most favorable conditions for aerobic dolomite precipitation occur at 35 °C, the temperature of optimal bacterial growth. The concentration of Sr in dolomite was found to be greater at higher experimental temperatures, in accordance with the higher miscibility of ions in minerals at higher temperatures. Further, the microbial dolomite with the highest Sr concentrations was precipitated in sulfate-rich cultures. We have demonstrated that the mechanism of Sr incorporation into the dolomite is most likely by adsorption or occlusion rather than by replacement of Ca by Sr. Thus, we conclude that the efficiency of Ca, Mg and Sr incorporation into dolomite, as well as the D_{Sr}^{dol}, is a function of temperature, bacteria metabolic activity and sulfate concentration. It remains essential, however, to determine the exact location of the Sr in the dolomite crystals, which is the goal of an ongoing study.

We propose that ancient and Recent dolomite with relatively high Sr concentrations are primary bacterial precipitates and not a secondary replacement of aragonite. Further, we propose that our results are in accordance with Land (1985), who proposed that (1) sedimentary dolomites with high Sr concentrations and low Fe concentrations may reflect precipitation under aerobic conditions and (2) dolomites with low Sr concentrations and high Fe concentrations may indicate precipitation under anaerobic conditions. We now recognize that both types could be products of microbial mediation. Indeed, Sr-rich dolomite suggests that the precipitation water had a greater salinity than normal seawater and a considerable sulfate concentration. We conclude that Sr may be an ideal indicator for the paleosalinity and paleotemperature of dolomite formation environments.

Finally, precipitation of dolomite, even biologically mediated, requires special conditions. In particular the medium should not be flowing water, but an organic colloi-

dal suspension. If the bacteria are immersed in this medium, the dispersion of metabolites, which create the favorable chemical conditions for dolomite precipitation, is drastically decreased. Moreover, this occurs adjacent to the active surface of the bacteria that can act as a nucleation site. Indeed, as the important role of microbial mediation in sedimentary carbonate processes becomes better understood, it will become necessary to reevaluate currently accepted geochemical paradigms associated with carbonate formations.

ACKNOWLEDGMENTS

The Swiss Science National Foundation (SNF) is gratefully acknowledged for generous financial support through Grant Nos. 20-067620 and 20-105149. This study also received support from the NASA's Astrobiology Institute, the European Science Foundation (ESF), ArchEnvironn-2650; 2503050-IPBSL from ERC and AYA-2009-11681 from MICINN (Spain). ASN acknowledges support from Grants CGL-2009-09249 and CGL-2007-66744-CO2-01 from MEC (Spain). Peter Swart is very much acknowledged for his constructive support on this work and for the extensive discussions. We acknowledge Patrick Meister for his extensive discussions and help in separating the biocrystals and the assistance of Michael Plötze with XRD. We also acknowledge the assistance of Thomas Pettke and Claudia Pudack with LA-ICP-MS analyses, and their kind assistance with interpreting the data. Finally, Robert H. Byrne, H. Catherine, W. Skinner and two anonymous reviewers provided comments that greatly improved the earlier version of this manuscript.

APPENDIX A. SUPPLEMENTARY DATA

Supplementary data associated with this article can be found, in the online version, at doi:10.1016/j.gca.2010.11.015.

REFERENCES

Arahal D. R., Marquez M. C., Volcani B. E., Schleifer K. H. and Ventosa A. (1999) *Bacillus marismortui* sp. nov., a new moderately halophilic species from the Dead Sea. *Int. J. Syst. Bacteriol.* **49**, 521–530.

Bader R. F. W. and Preston H. J. T. (1966) A critique of Pauli repulsions and molecular geometry. *Can. J. Chem.* **44**, 1131–1145.

Bader R. F. W. (2006) Pauli repulsions exist only in the eye of the beholder. *Chem. Eur. J.* **12**, 2896–2901.

Baker P. A. and Burns S. J. (1985) Occurrence and formation of dolomite in organic-rich continental margin sediments. *Am. Assoc. Petrol. Geol. Bull.* **69**, 1917–1930.

Banner J. L., Wasserburg G. J., Chen J. H. and Humphrey J. D. (1991) Uranium-series evidence on diagenesis and hydrology in Pleistocene carbonates of Barbados, West Indies. *Earth Planet. Sci. Lett.* **107**, 129–137.

Bein A. and Land L. S. (1983) Carbonate sedimentation and diagenesis associated with Mg–Ca-chloride brines: The Permian San Andres formation in the Texas Panhandle. *J. Sediment. Petrol.* **53**, 243–260.

Behrens E. W. and Land L. S. (1972) Subtidal Holocene dolomite, Baffin Bay, Texas. *J. Sediment. Petrol.* **42**, 155–161.

Botz R. W. and von der Borch C. C. (1984) Stable isotope study of carbonate sediments from the Coorong area, South Australia. *Sedimentology* **31**, 837–849.

Braissant O., Callileau G., Dupraz C. and Verecchia E. P. (2003) Bacterially induced mineralization of calcium carbonate in terrestrial environments: the role of expolysaccharides and amino acids. *J. Sediment. Res.* **73**, 485–490.

De Deckker P. (1988) Biological and sedimentary facies of Australian salt lakes. *Paleogeogr. Paleoclimatol. Palaeoecol.* **62**, 237–270.

Dromgoole E. L. and Walter L. M. (1990) Inhibition of calcite growth-rates by Mn^{2+} in $CaCl_2$ solutions at 10 °C, 25 °C and 50 °C. *Geochim. Cosmochim. Acta* **54**, 2991–3000.

Faison B. D., Cancel C. A., Lewis S. N. and Howard H. I. (1990) Binding of dissolved strontium by *Micrococcus luteus*. *Appl. Environ. Microbiol.* **56**, 3649–3656.

Ferris F. G., Fyfe W. S. and Beveridge T. J. (1991) Bacteria as nucleation sites for authigenic minerals. In *Diversity of Environmental Geochemistry. Development in Geochemistry*, vol. 6 (ed. J. Berthelin). Amsterdam, Elsevier, pp. 319–326.

Friis A. K., Davis T. A., Figueira M. M., Paquette J. and Mucci A. (2003) Influence of *Bacillus subtilis* cell walls and EDTA on calcite dissolution rates and crystal surface features. *Environ. Sci. Technol.* **37**, 2376–2382.

Garcia del Cura M. A., Calvo J. P., Ordoñez S., Jones B. F. and Canaveras J. C. (2001) Petrographic and geochemical evidence for the formation of primary, bacterially induced lacustrine dolomite, La Roda 'white earth' (Pliocene, central Spain). *Sedimentology* **48**, 897–915.

Guenther D., Frischkencht R., Heinrich C. and Kahlert H. (1997) Capabilities of an argon fluoride 193 nm excimer laser for laser ablation inductively coupled plasma mass spectrometry microanalysis of geological materials. *J. Anal. Atom. Spectrom.* **12**, 939–944.

Guenther D. and Heinrich C. (1999) Enhanced sensitivity in laser ablation-ICP mass spectrometry using helium–argon mixtures in aerosol carrier. *J. Anal. Atom. Spectrom.* **14**, 1363–1368.

Henderson L. M. and Kracek F. C. (1927) The fractional precipitation of barium and radium chromates. *J. Am. Chem. Soc.* **49**, 739–749.

Hood S. D., Nelson C. S. and Kamp P. J. J. (2004) Burial dolomitization in a non-tropical carbonate petroleum reservoir: the Oligocene Tikorangi Formation, Taranaki Basin, New Zealand. *Sediment. Geol.* **172**, 117–138.

Humphrey J. D. (1988) Late Pleistocene mixing zone dolomitization, southeastern Barbados, West Indies. *Sedimentology* **35**, 327–328.

Hurtgen M. T., Galen G. P., Arthur M. A. and Hoffman P. F. (2006) Sulfur cycling in the aftermath of 635-Ma snowball glaciation: evidence for a syn-glacial sulfidic deep ocean. *Earth Planet. Sci. Lett.* **245**, 551–570.

Ingerson E. (1962) Problems of the geochemistry of sedimentary carbonate rocks. *Geochim. Cosmochim. Acta* **26**, 815–847.

James S. R., Dobson S. J., Franzmann P. D. and McMeekin T. A. (1990) *Halomonas meridiana*, a new species of extremely halotolerant bacteria isolated from Antarctic saline lakes. *Syst. Appl. Microbiol.* **13**, 270–277.

James N. P., Narbonne G. M. and Kyser T. K. (2001) Late Neoproterozoic cap carbonates: Mackenzie Mountains, northwestern Canada: Precipitation and global glacial meltdown. *Can. J. Earth Sci.* **38**, 1229–1262.

Katz A., Starinsk A., Sass E. and Holland H. D. (1972) Strontium behavior in aragonite–calcite transformation – experimental study at 40–98 °C. *Geochim. Cosmochim. Acta* **36**, 481–496.

Katz A. (1973) Interaction of magnesium with calcite during crystal growth at 25–90 °C and 1 atm. *Geochim. Cosmochim. Acta* **37**, 1563–1586.

Katz A. and Mathews A. (1977) The dolomitization of $CaCO_3$: an experimental study at 252–295 °C. *Geochim. Cosmochim. Acta* **41**, 297–308.

Kelts K. and McKenzie J. A. (1982) Diagenetic dolomite formation in Quaternary anoxic diatomaceous muds of DSDP Leg 64, Gulf of California. *Initial Reports of the Deep Sea Drilling Project* **64**(Part 2), 553–569.

Klug H. P. and Alexander L. E. (1973) *X-ray Diffraction Procedures for Polycrystalline and Amorphous Materials*. John Wiley and Sons, New York, p. 965.

Kretz R. (1982) A model for the distribution of trace elements between calcite and dolomite. *Geochim. Cosmochim. Acta* **46**, 1979–1981.

Land L. S. (1973) Holocene meteoric dolomitization of Pleistocene limestones, North Jamaica. *Sedimentology* **20**, 411–424.

Land L. S. and Hoops G. K. (1973) Sodium in carbonate sediments and rocks, a possible index to the salinity of diagenetic solutions. *J. Sediment. Petrol.* **43**, 614–617.

Land L. S., Salem M. R. I. and Morrow D. W. (1975) Paleohydrology of ancient dolomites: geochemical evidence. *Am. Assoc. Petrol. Geol. Bull.* **59**, 1602–1625.

Land L. S. (1980) The isotopic and trace-element geochemistry of dolomite: The state of the art. In *Concepts and models for dolomitization. Soc. Econ. Paleontol. Mineral. Spec. Publ.* **28** (eds. D.H. Zenger, J.B. Duhman, and R.L. Ethington), pp. 87–110.

Land L. S. (1985) The origin of massive dolomite. *J. Geol. Educ.* **33**, 112–125.

Land L. S. (1998) Failure to precipitate dolomite at 25 °C from dilute solution despite 1000-fold oversaturation after 32-years. *Aquatic. Geochem.* **4**, 361–368.

Longerich H. P., Jackson S. E. and Gunther D. (1996) Laser ablation inductively coupled plasma mass spectrometric transient signal data acquisition and analyte concentration calculation. *J. Anal. Atom. Spectrom.* **11**, 899–904.

Lumsden D. N. (1979) Discrepancy between thin-section and X-ray estimates of dolomite in limestone. *J. Sediment. Petrol.* **49**, 429–435.

Malone M. J., Baker P. A. and Burns S. J. (1994) Recrystallization of dolomite: evidence from the Monterey Formation (Miocene), California. *Sedimentology* **41**, 1223–1239.

Malone M. J., Baker P. A. and Burns S. J. (1996) Recrystallization of dolomite: an Experimental study from 50–200 °C. *Geochim. Cosmochim. Acta* **60**, 2189–2207.

Martín, J. D. (2004) Using XPowders a software package for powder X-ray diffraction analysis. D.L. GR-1001/04, ISBN: 84-609-1497-6, Spain. Available from: <http://www.xpowder.com>.

Mastandrea A., Perri E., Russo F., Spadafora A. and Tucker M. (2006) Microbial primary dolomite from a Norian carbonate platform: northern Calabria, southern Italy. *Sedimentology* **53**, 465–480.

Mazzullo S. J., Bischoff W. D. and Teal C. S. (1995) Holocene shallow-subtidal dolomitization by near-normal seawater, northern Belize. *Geology* **23**, 341–344.

McIntire W. L. (1963) Trace element partition coefficients – a review of theory and applications to geology. *Geochim. Cosmochim. Acta* **27**, 1209–1264.

Meister P., McKenzie J. A., Vasconcelos C., Bernasconi S., Frank M., Gutjahr M. and Schrag D. P. (2007) Dolomite formation in the dynamic deep biosphere: results from the Peru Margin. *Sedimentology* **54**, 1007–1031.

Moreira N. F., Walter L. M., Vasconcelos C., McKenzie J. A. and McCall J. P. (2004) Role of sulfide oxidation in dolomitization: sediment and pore-water geochemistry of a modern hypersaline lagoon system. *Geology* **32**, 701–704.

Morita R. Y. (1980) Calcite precipitation by marine bacteria. *Geomicrobiol. J.* **2**, 63–82.

Müller G. and Wagner F. (1978) Holocene carbonate evolution in Lake Balaton (Hungary): a response to climate and the impact of man. In *Modern and Ancient Lakes Sediment. Int. Assoc. Sediment. Spec. Pub*, vol. 2 (eds. A. Matter and M. E. Tucker). Blackwell Scientific Publications, Oxford, pp. 57–81.

Nernst W. (1891) Verteilung eines Stoffes zwischen zwei Lösungsmitteln und zwischen Lösungsmittel und Dampfraum. *Zeitsch. Phys. Chem.* **8**, 110–139.

Ohde S. and Kitano Y. (1981) Protodolomite in Dajito-Jima, Okinawa. *Geochem. J.* **15**, 199–207.

Reeder R. J., Lamble G. M. and Northrup P. A. (1999) XAFS study of the coordination and local relaxation around Co^{2+}, Zn^{2+}, Pb^{2+}, and Ba^{2+} trace elements in calcite. *Am. Mineral.* **84**, 1049–1060.

Reeder R. J., Elzinga E. J. and Rouff A. (2002) Coordination of some metals sorbed at the calcite–water interface. *Geochim. Cosmochim. Acta* **66**, A628.

Roberts J. A., Bennett P. C., Gonzalez L. A., Macpherson G. L. and Miliken K. L. (2004) Microbial precipitation of dolomite in methanogenic groundwater. *Geology* **32**, 277–280.

Rosen M. R., Miser D. E. and Warren J. K. (1988) Sedimentology, mineralogy and isotopic analysis of Pellet Lake, Coorong Region, South Australia. *Sedimentology* **35**, 105–122.

Sánchez-Román M., Rivadeneyra M., Vasconcelos C. and McKenzie J. A. (2007) Biomineralization of carbonate and phosphate by halophilic bacteria: influence of Ca^{2+} and Mg^{2+} ions. *FEMS Microbiol. Ecol.* **61**, 273–284.

Sánchez-Román M., Vasconcelos C., Schmid T., Dittrich M., McKenzie J. A., Zenobi R. and Rivadeneyra M. A. (2008) Aerobic microbial dolomite at the nanometer scale: implications for the geologic record. *Geology* **36**, 879–882.

Sánchez-Román M., Vasconcelos C., Warthmann R., Rivadeneyra M. A. and McKenzie J. A. (2009a) Microbial dolomite precipitation under aerobic conditions: results from Brejo do Espinho Lagoon (Brazil) and culture experiments. *Int. Assoc. Sediment. Spec. Publ.* **40**, 167–178.

Sánchez-Román M., McKenzie J. A., de Luca Rebello Wagener A., Rivadeneyrac M. A. and Vasconcelos C. (2009b) Presence of sulfate does not inhibit low-temperature dolomite precipitation. *Earth Planet. Sci. Lett.* **285**, 131–139.

Stumm W. and Morgan J. J. (1996) *Aquatic chemistry: Chemical Equilibria and Rates in Natural Waters*, third ed. Wiley Interscience, New York, p. 780.

Sun S. S. and Hanson G. N. (1975) Origin of Ross island basanitoids and limitations on the heterogeneity of mantle sources of alkali basalts and nephelinites. *Contrib. Mineral. Petrol.* **54**, 77–106.

Vahrenkamp V. C. and Swart P. K. (1990) New distribution coefficient for the incorporation of strontium into dolomite and its implications for the formation of ancient dolomites. *Geology* **18**, 387–391.

Valero B. L. and Gisbert J. (1994) Permian saline lakes in the Aragon-Bearn basin, western Pyrenees. In *Sedimentology and Geochemistry of Modern and Ancient Saline Lakes* (eds. R. W. Renaut and W. M. Last). *Soc. Econ. Paleontol. Mineral. Spec. Publ.* **50**, 267–290.

van Lith Y., Vasconcelos C., Warthmann R. and McKenzie J. A. (2003a) Sulphate-reducing bacteria induce low-temperature Ca-dolomite and high Mg-calcite formation. *Geobiology* **1**, 71–79.

van Lith Y., Warthmann R., Vasconcelos C. and McKenzie J. A. (2003b) Microbial fossilization in carbonate sediments: a result of the bacterial surface involvement in dolomite precipitation. *Sedimentology* **50**, 237–245.

Vasconcelos C. and McKenzie J. A. (1997) Microbial mediation of modern dolomite precipitation and diagenesis under anoxic

conditions (Lagoa Vermelha, Rio de Janeiro, Brazil). *J. Sediment. Res.* **67**, 378–390.

Vasconcelos C., McKenzie J. A., Warthmann R. and Bernasconi S. (2005) Calibration of $\delta^{18}O$ paleothermometer for dolomite precipitated in microbial cultures and natural environments. *Geology* **33**, 317–320.

Videtich P. E. (1982) Origin, marine diagenesis, and early freshwater diagenesis of limestones and dolomite (Tertiary-Recent): stable isotopic, electron microprobe and petrographic studies. Ph. D. Thesis, Brown University.

Warthmann R., van Lith Y., Vasconcelos C., McKenzie J. A. and Karpoff A. M. (2000) Bacterially induced dolomite precipitation in anoxic culture experiments. *Geology* **28**, 1091–1094.

Weber J. N. (1964) Trace element composition of dolostones and dolomites and its bearing on the dolomite problem. *Geochim. Cosmochim. Acta* **28**, 1817–1868.

Wright D. T. (1999) The role of sulphate-reducing bacteria and cyanobacteria in dolomite formation in distal ephemeral lakes of the Coorong region, South Australia. *Sediment. Geol.* **126**, 147–157.

Wright D. T. and Wacey D. (2005) Precipitation of dolomite using sulphate-reducing bacteria from the Coorong Region, South Australia: significance and implications. *Sedimentology* **52**, 987–1008.

Zen E. A. (1960) Carbonate equilibria in the open ocean and their bearing on the interpretations of ancient carbonate rocks. *Geochem. Cosmochim. Acta* **18**, 57–71.

Associate editor: Robert H. Byrne